NASA TECHNICAL MEMORANDUM

NASA TM-73782

NASA TM-73782

FRICTION AND WEAR BEHAVIOR OF SINGLE-CRYSTAL SILICON CARBIDE IN SLIDING CONTACT WITH VARIOUS METALS

by Kazuhisa Miyoshi and Donald H Buckley
Lewis Research Center
Cleveland, Ohio 44135

TECHNICAL PAPER to be presented at the
Annual Meeting of American Society of Lubrication Engineers
Dearborn, Michigan, April 17-20, 1978

FRICTION AND WEAR BEHAVIOR OF SINGLE-CRYSTAL SILICON CARBIDE IN SLIDING CONTACT WITH VARIOUS METALS

by Kazuhisa Miyoshi and Donald H. Buckley

National Aeronautics and Space Administration
Lewis Research Center
Cleveland, Ohio 44135

E-9337

ABSTRACT

Sliding friction experiments were conducted with single-crystal silicon carbide in contact with various metals. Results indicate the coefficient of friction is related to the relative chemical activity of the metals. The more active the metal, the higher the coefficient of friction. All the metals examined transferred to silicon carbide. The chemical activity of the metal and its shear modulus may play important roles in metal-transfer, the form of the wear debris and the surface roughness of the metal wear scar. The more active the metal, and the less resistance to shear, the greater the transfer to silicon carbide and the rougher the wear scar on the surface of the metal. Hexagon-shaped cracking and fracturing formed by cleavage of both prismatic and basal planes is observed on the silicon carbide surface.

INTRODUCTION

Silicon carbide has been used and has great potential for use in high-hardness and/or temperature applications such as a stable high-temperature semiconductors, turbine ceramic seal systems, and as an abrasive for grinding. The present authors have conducted experimental work to determine the tribophysical properties of single-crystal silicon carbide. This work has included a determination of (a) the friction and wear behavior of silicon carbide in contact with itself and with titanium (ref. 1), (b) the friction, deformation, and fracture behavior of silicon carbide in contact with diamond, and (c) the influence of the crystallographic orientation of silicon carbide on its friction and deformation (ref. 2).

The present investigation was conducted to examine the friction and wear behavior of single-crystal silicon carbide in contact with various metals and to examine the nature of interaction of silicon carbide wear debris and metal-

transfer to silicon carbide. Experiments were conducted with loads of 5 to 50 grams at a sliding velocity of 3 millimeters per minute in a vacuum of 10^{-8} N/m^2 and at 25° C on the silicon carbide (0001) basal plane in the $\langle 10\bar{1}0 \rangle$ directions. The metals were all polycrystalline.

MATERIALS

The single-crystal silicon carbide platelets used in these experiments were a 99.9-percent pure compound of silicon and carbon (table I(a)). Silicon carbide has a hexagonal close-packed crystal structure. The C direction was perpendicular to the sliding interface with the basal plane therefore parallel to the interface. The Knoop hardness was 2954 in the $\langle 10\bar{1}0 \rangle$ and 2917 in the $\langle 11\bar{2}0 \rangle$ directions on the basal plane of silicon carbide (ref. 6).

The metals were all polycrystalline. The titanium was 99.97 percent pure, the copper was 99.999 percent pure, and all the other metals were 99.99 percent pure (table I(b)).

EXPERIMENTAL APPARATUS AND PROCEDURE

Apparatus

The apparatus used in the investigation was a vacuum system capable of measuring adhesion, load, and friction. The apparatus also contained tools for surface analysis, an Auger emission spectrometer, and a LEED (low-energy electron diffraction system). The mechanism used for measuring adhesion, load, and friction is shown schematically in figure 1. A gimbal-mounted beam was projected into the vacuum system. The beam contained two flats machined normal to each other with strain gages mounted thereon. The end of the rod contained the metal pin specimen. As the beam was moved normal to the disk, a load was applied and was measured by the strain gage. The vertical sliding motion of the pin along the disk surface was accomplished through a motorized gimbal assembly. The friction force was sensed with a strain gage normal to that used to measure load. Multiple wear tracks could be generated on the disk specimen surface by translational motion of the beam containing the pin. This feature was used to examine the coefficient of friction at various loads. Pin

sliding was in the vertical direction as shown in figure 1. The electron beam from both LEED and Auger spectroscopy systems incorporated in the apparatus could be focused on any disk site desired.

Experimental Procedure

The disk flat (silicon carbide) and metal pin specimens were polished with diamond powder and with aluminum oxide (Al_2O_3) powder. Both powders had particle diameters of 3 and 1 micrometers. The radius of the pin specimens was 0.79 millimeter. The surfaces of the disk and pin specimens were rinsed with absolute ethyl alcohol before the experiment.

For the experiments in vacuum, the specimens were placed in the vacuum chamber and the system evacuated and baked out to achieve a pressure of 1.33×10^{-8} N/m^2 (10^{-10} torr). When this vacuum was achieved, argon gas was bled back into the vacuum chamber to a pressure of 1.3 N/m^2. A 1000-volt, direct-current potential was applied and the specimens (both disk and rider) were argon sputter bombarded for 30 minutes. After 1 hour, the vacuum chamber was reevacuated and Auger spectra of the disk surface were obtained to determine the degree of surface cleanliness. When the disk surface was clean, friction experiments were conducted.

Loads of 5 to 50 grams were applied to the pin-disk contact by deflecting the beam of figure 1. Both load and friction force were continuously monitored during a friction experiment. Sliding velocity was 3 millimeters per minute with a total sliding distance of 2.5 millimeters. All friction experiments in vacuum were conducted with the system reevacuated to a pressure of 10^{-8} N/m^2.

RESULTS AND DISCUSSION

Friction Behavior

Sliding friction experiments were conducted with single-crystal silicon carbide in contact with various metals shown in table I(b). There were no changes in coefficient of friction with load. The friction traces were primarily characterized by marked stick-slip behavior over the entire load range with all the

metals. This type of friction is anticipated where strong adhesion occurs at the interface.

The relative chemical activity of the transition metals (metals with partially filled d shells) as a group can be ascertained from their percent d bond character after Pauling (ref. 9). Adhesion and friction properties of the transition metals sliding on metals have been shown to be related to this property (ref. 10). The greater the percent d bond character, the less active is the metal and the less the coefficient of friction. Whether a similar concept applies to the interactions of ceramic-to-metal interfaces is a matter of interest.

The average coefficient of friction over an entire range of loads for a number of transition metals in sliding contact with single-crystal silicon carbide are presented in figure 2 as function of the d bond character of the transition metal. The data of figure 2 indicate a decrease in friction with an increase in d character of the metallic bond. There appears to be very good agreement between friction and chemical activity of the transition metals.

Aluminum and copper both have a chemical affinity for silicon and carbon. Their affinity for silicon is not as great as for carbon. Copper is, however, less chemically active with respect to both silicon and carbon indicating that it does not have as strong a chemical affinity or tendency to bond to these elements as does aluminum (ref. 11).

Data were obtained for aluminum and copper sliding on single-crystal silicon carbide. Coefficients of friction as function of load are presented in figure 3. Examination of figure 3 indicates no change in coefficient of friction with load, as mentioned above. The average coefficient of friction is approximately 0.57 with aluminum. It is almost the same as that for silicon carbide in sliding on the more chemically active metal titanium and with silicon carbide itself (see fig. 3). It is, however, greater than that for copper sliding on silicon carbide where the coefficient of friction is approximately 0.40. Higher friction is observed with the chemically more active metal aluminum. Thus, the chemical

activity of a metal plays a role in adhesion and friction of single-crystal silicon carbide contacting metals.

Metal-Transfer

All the silicon carbide surfaces contacted by the metals investigated were found to have transferred metal even with a single pass of the metal rider.

When repeated passes were made of the metal riders over the same single-crystal silicon carbide surface, the coefficient of friction generally decreased with number of passes to an equilibrium value which seemed to depend on the nature of transfer of the metals. In contrast, when repeated passes were made with the silicon carbide rider on silicon carbide, the coefficient of friction was generally constant. The type of metal-transfer to silicon carbide was generally governed for the four different groups of metals by two factors: (1) chemical affinity of metal for silicon and carbon and (2) resistance to shear of the metal, that is, the shear modulus.

Aluminum and titanium. - Aluminum and titanium, having much stronger chemical affinity for silicon and carbon, exhibited considerably high friction. However, they have the least resistance to shear. Sliding of these metals on silicon carbide results in a copious amount of transfer of them to silicon carbide.

Figure 4 presents scanning electron micrographs and an X-ray map of a wear track, generated by a single pass of the aluminum rider. It becomes obvious from figure 4 that the copious amount of aluminum transfers to the silicon carbide in a single pass of the rider. In figure 4(a) the light area in the midsection of the figure, where aluminum transfer is evident, was the contact area before gross sliding of rider. It is the area where the surfaces of metal and silicon carbide were sticking together, as schematically shown in figures 5(a) to (c). That is, where both loading and tangential forces were applied to the specimens, but before gross sliding had occurred large amounts of aluminum transferred to the silicon carbide. The top of figure 4(a) is the area, where less aluminum transfer is evident, after gross sliding of rider, and the surfaces of metal and silicon carbide were in a rapid slip. Note that, in an X-ray energy dispersive

analysis for aluminum on the silicon carbide surface shown in figure 4(b), the concentrations of white spots correspond to those locations in figure 4(a) where copious amount of aluminum transferred. Thus, fracture of cohesive bonds in aluminum occurs during sliding, and the presence of copious amounts of aluminum transfer is in the sticking area where strong adhesion occurs at the interface. Detailed examination of aluminum transfer to the silicon carbide, in figure 4(c), clarifies the two types of aluminum wear debris generated by fracture of cohesive bonds of aluminum. One type is cylindrical particles where the direction of the cylinder is perpendicular to the sliding direction. The second type is a thin film which is streaky and perpendicular to the sliding direction.

Following examination of a wear track generated by a single pass of the rider a wear track was generated by multipasses of the aluminum rider. Figure 6 presents a scanning electron micrograph and an aluminum K_{α} X-ray map of the point of beginning of a wear track on the silicon carbide, generated by 10 passes of the aluminum rider over the same silicon carbide surface. It is obvious from figure 6 that the aluminum transfer is much more than that obtained with a single pass of the aluminum rider shown in figure 4. Further, figure 6 reveals that multilayer film structure of aluminum transfer was produced by multicontacting and sliding, as schematically shown in figures 5(d) to (f). The multilayer film structure is due to piling up of aluminum wear debris.

Aluminum, generally, produced four types of wear debris with aluminum multipass sliding on silicon carbide: (1) a very thin transfer film on the entire contact area, (2) multilayer transfer films, (3) very small particles (submicron in size), and (4) piled-up particles (several micrometers in size). In addition to the four types of aluminum wear debris or transfer, cylindrical particles shown in figure 4, were detected on the silicon carbide surface.

Examination of wear tracks on the silicon carbide after single pass sliding with titanium revealed evidence of both very thin transfer films and lump particles of titanium transferred to the silicon carbide (ref. 1). On the other hand, examination of the silicon carbide surface after multipass sliding with titanium

indicated the presence of very thin transfer films, multilayer transfer films, very small particles, and pile-up of particles. Thus, the wear debris of titanium transferred to the silicon carbide is very similar to that observed with aluminum.

Nickel, copper, and cobalt. - Nickel, copper, and cobalt have less chemical affinity for silicon and carbon and greater resistance to shear than have aluminum and titanium.

Generally, nickel, copper, and cobalt produced the three types of wear debris, that is, very thin transfer films, very small particles, and piled-up particles. Nickel produced more transfer of thin films than did copper and cobalt. This appeared to be related to the lower coefficient of friction that was observed for copper and cobalt. With nickel the coefficient of friction was approximately 0.48, with copper 0.40, and with cobalt 0.42. The amount of transfer for nickel, copper, and cobalt to silicon carbide was less than was observed with aluminum and titanium.

Iron. - Iron appears to have almost the same chemical affinity for silicon and carbon as nickel but has a greater resistance to shear. There were very small particles and piled-up particles, but there was very little evidence for a thin transfer film on the wear track. This is apparently related to the greater resistance to shear of iron compared to nickel or copper.

Rhodium and tungsten. - Rhodium and tungsten have the least chemical affinity for silicon and carbon and the greatest resistance to shear of all metals investigated. Large lumps (several micrometers in size) and very small wear particles (submicron in size) of rhodium and tungsten transferred to silicon carbide. A few lump particles were deformed plastically during multipasses sliding.

Rhodium and tungsten can be characterized as producing and transferring lumps of wear particles to silicon carbide as a result of sliding. This may be due to the greater shear moduli of tungsten and rhodium.

Comparison of metal-transfer. - Table II summarizes metal-transfer to single-crystal silicon carbide observed after multiple passes sliding. Generally,

metals farther to the right in table II have less chemical affinity for silicon and carbon, lower coefficient of friction, and greater resistance to shear. Therefore, with metals (exceptions rhodium and tungsten) further to the right in table II, less transfer to silicon carbide was observed. Tungsten and rhodium had the greatest resistance to shear and produce lump wear particles, which were quite different from the wear debris observed for other metals.

Wear Behavior

Single-crystal silicon carbide. - The sliding of a metal rider on silicon carbide results in cracks along cleavage planes of $\{10\bar{1}0\}$. Figure 7 shows scanning electron micrographs of the wear tracks on silicon carbide surfaces generated by 10 passes of rhodium and copper riders, respectively. The cracks, which are observed in the wear tracks, primarily propagate along cleavage planes of $\{10\bar{1}0\}$. In figure 7(a), a hexagon-shaped light area at the beginning of wear track is a large cracking where the cracks were generated, propagated and then intersected during loading and sliding of the rhodium rider. It is anticipated from figure 7(a) that subsurface-cleavage cracking of (0001) planes also occurs. Figure 7(b) indicates the surface cracking observed on the side of the wear track, along cleavage planes of $\{10\bar{1}0\}$. Figure 8 reveals the wear tracks are accompanied by nearly complete hexagon-shaped pits. Wear debris particles as seen in figure 7 have been already ejected from the wear track. Again, the fracture is primarily due to the surface cracking of $\{10\bar{1}0\}$ planes and subsurface cracking of (0001) planes, parallel to the interface as anticipated. Scanning electron micrographs and an X-ray energy dispersive analysis for titanium on the silicon carbide surfaces are shown in figures 8(a) and (b). The concentrations of white spots in figure 8(b) correspond to those locations in figure 8(a) where titanium transfer is evident. The copious amount of thin titanium film was seen around the hexagon-shaped pits in figure 8(a). These figures indicate that the cohesive bonds of both the silicon carbide and titanium fractured near the strong adhesive bonds at the interface.

Dislodged gross wear particle of silicon carbide, with their fracture surfaces exposed, had copious amounts of titanium on their back as shown in figure 9. Figure 9 presents a scanning electron micrograph and an X-ray energy-dispersive analysis of silicon carbide wear track. Thus, fracture may occur in silicon carbide near the interfacial adhesive bond and silicon carbide wear debris particles are formed.

Metals. - The wear scar on the metal rider after it slid against silicon carbide showed evidence of a large number of plastically deformed grooves and indentations which depended on the nature of transfer for silicon carbide and metal. They were formed primarily by sliding and rolling of silicon carbide wear debris.

The wear scars of aluminum and titanium, which have much stronger chemical affinity to silicon and carbon and less resistance to shear, are generally rougher than with the other metals investigated (copper, nickel, cobalt, and iron). The titanium wear scar has the roughest surface. This may be because of the large amount of silicon carbide that transfers to titanium (ref. 1).

Rhodium and tungsten have the greatest resistance to shear of all the metals investigated. The wear scar on rhodium shows evidence of a fractured surface in addition to plastically deformed grooves and indentations. These are primarily produced by sliding and rolling of silicon carbide wear debris, as shown in figure 10(a). Further, with rhodium a significant degree of cracking initiates in grain boundaries and extends along them. Such a crack is shown in the scanning electron micrograph of figure 10(b).

Tungsten also showed the fractured surface and cracking along grain boundaries. The fracturing and cracking of rhodium and tungsten may be primarily due to their greater shear moduli.

Metal wear scars, then, with the exception of rhodium and tungsten further to the left in table II are generally rougher.

Nature of Interaction on Silicon Carbide Wear Debris

The wear scars on metals after sliding on silicon carbide surfaces may contain silicon carbide wear debris, as shown in figures 11(a) to (c). Figures 11(a)

to (c) indicate that the wear debris of silicon carbide, produced in sliding, transferred (was embedded) to the metal riders. The wear debris generally slides and/or rolls on the metal surfaces, and produces the indentations and deep grooves shown in figures 11(b) and (c). Figure 11(b) shows straight grooves, along the sliding direction on the metal, formed by sliding of silicon carbide wear debris. Figure 11(c) also shows straight rows of indentations, along the sliding direction, formed by rolling of silicon carbide wear debris.

In addition, figure 12 reveals that silicon carbide wear debris produced by friction, plowed the silicon carbide surface itself, and the grooves are produced in a plastic manner on the surface of silicon carbide. Generally, the silicon carbide wear debris particle is covered with a metal film as indicated in the X-ray map of figure 12(b).

CONCLUSIONS

The following conclusions are drawn from the data presented herein:

1. The coefficient of friction for silicon carbide sliding on various metals is related to the relative chemical activity of those metals. The more active the metal, the higher the coefficient of friction.

2. All the metals examined transferred to the surfaces of silicon carbide on sliding. The chemical affinity of metal to silicon and carbon and the shear modulus of the metal play important roles in metal transfer and the form of the wear debris. The less active and the greater resistance to shear the metal (except rhodium and tungsten), the less transfer to silicon carbide. Aluminum and titanium, having much stronger chemical affinity to silicon carbide and less resistance to shear than the other metals exhibited the greatest amount of transfer. Rhodium and tungsten have the greatest resistance to shear, and therefore produce and transfer lump wear particles.

3. The wear scars of aluminum and titanium, which have much stronger chemical affinity and less resistance to shear than copper, nickel, cobalt, and iron are generally rougher.

4. The hexagon-shaped cracking and fracturing of the single-crystal silicon carbide is due to cleavage of both prismatic and basal planes.

5. The silicon carbide wear debris produced by brittle fracture produces grooves and indentations on the surfaces of both the metal and silicon carbide itself.

REFERENCES

1. Miyoshi, K.; and Buckley, D. H.: Friction and Fracture of Single-Crystal Silicon Carbide in Contact with Itself and Titanium. ASLE Transactions in process.
2. Miyoshi, K.; and Buckley, D. H.: Friction, Deformation and Fracture of Single-Crystal Silicon Carbide. ASLE Transactions in process.
3. Taylor, A.; and Laidler, D. S.: The Formation and Crystal Structure of Silicon Carbide. Brit. J. Appl. Phys., 1 (1950), pp. 174-181.
4. Drowart, J.; and Maria, G. De: Thermodynamic Study of the Binary System Carbon-Silicon Using a Mass Spectrometer. Proceedings of the Conference on Silicon Carbide, O'Connor, J. R. and Smiltems, J., eds., Pergamon Press, New York, 1960, pp. 16-23.
5. Canahan, R. D.: Elastic Properties of Silicon Carbide. J. Amer. Ceram. Soc., 51, 1968, pp. 223-224.
6. Shaffer, P. T. B.: Effect of Crystal Orientation on Hardness of Silicon Carbide. J. Amer. Ceram. Soc., 47, 1964, p. 466.
7. Barrett, C. S.: Structure of Metals. McGraw-Hill Book Co., Inc., 1943, pp. 552-554.
8. Gschneider, K. A., Jr.: Physical Properties and Interrelationships of Metallic and Semimetallic Elements. Solid State Physics, vol. 16. Frederick Seitz and David Turnbull, eds., Academic Press, 1965, pp. 275-426.
9. Pauling, L.: A Resonating-Valence-Bond Theory of Metals and Intermetallic Compounds. Proc. Roy. Soc. A196, 1949, pp. 343-362.

10. Buckley, D. H.: The Metal-to-Metal Interface and its Effect on Adhesion and Friction - Journal of Colloid and Interface Science, 58, 1, 1977, pp. 36-53.

11. Brewer, L., et al.: Thermodynamic and Physical Properties of Nitrides, Carbides, Sulfides, Silicides, and Phosphides. "The Chemistry and Metallurgy of Miscellaneous Materials, Thermodynamics." Quill, L. L., ed., McGraw-Hill Book Co., Inc. (1950), pp. 40-59.

TABLE I. - CRYSTALLINE, PHYSICAL AND CHEMICAL PROPERTIES OF SPECIMENS

(a) Single-crystal silicon carbide specimen

Material	Purity, percent (a)	Crystal structure at 25° C	Lattice constants, Å (b)	Cohesive energy kcal/mole (c)	Shear modulus, 10^6 kg/cm^2 (d)
SiC	99.9	Hexagonal close-packed	a = 3.0817 c = 15.1183 c/a = 4.9058	125±3	2.04 (200 GN/m^{-2})

(b) Metal specimens

Metal	Purity, percent (a)	Crystal structure at 25° C (e)	Lattice constants, Å (e)	Cohesive energy, kcal/(g)(atom) (f)	Shear modulus, 10^6 kg/cm^2 (f)	Percent d character for transition elements (g)
Tungsten	99.99	Body-centered cubic	a = 3.1586	199.7	1.56±0.04	43
Iron	99.99	Body-centered cubic	a = 2.8610	99.4	0.831±0.006	39.7
Rhodium	99.99	Face-centered cubic	a = 3.7956	133.0	1.50±0.03	50
Nickel	99.99	Face-centered cubic	a = 3.5169	102.3	0.765	40.0
Titanium	99.97	Hexagonal close-packed	a = 2.953 c = 4.729 c/a = 1.587	112.2	0.401±0.005	27
Cobalt	99.99	Hexagonal close-packed	a = 2.507 c = 4.072 c/a = 1.624	101.7	0.779	39.5
Copper	99.999	Face-centered cubic	a = 3.6080	80.8	0.460±0.015	----
Aluminum	99.99	Face-centered cubic	a = 4.0414	76.9	0.271±0.001	----

[a]Manufacturer's analysis.

[b]From ref. 3.

[c]From ref. 4, heat of formation in kcal/mole of gaseous silicon and graphite from hexagonal silicon carbide.

[d]From ref. 5.

[e]From ref. 7.

[f]From ref. 8.

[g]From ref. 9.

TABLE II. - METAL-TRANSFER TO SINGLE-CRYSTAL SILICON CARBIDE (0001) SURFACE AS A RESULT OF MULTIPLE PASS SLIDING

Form of metal transfer	Metals[a]							
	Al	Ti	Cu	Ni	Co	Fe	Rh	W
Very small particle (submicron in size)	+	+	+	+	+	+	+	+
Piled-up particle (several microns in size)	+	+	+	+	+	+	-	-
Streak thin film	+	+	+	+	+	-	-	-
Multilayer film structure (piled up)	+	+	-	-	-	-	-	-
Lump particle (several microns in size)	(+)	(+)	-	-	-	-	+	+
Surface roughness of metal wear scar	← Rougher							
Chemical affinity of metal for silicon and carbon	→ Lesser							
Resistance to shear of metal	→ Greater							

[a]Transferred after 10 passes sliding +; not transferred after 10 passes sliding - ; transferred after single pass sliding (+)

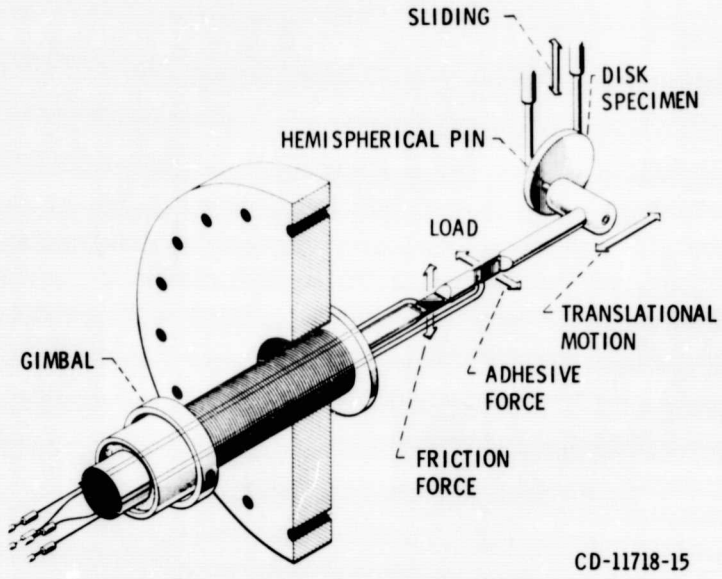

Figure 1. - High-vacuum friction and wear apparatus.

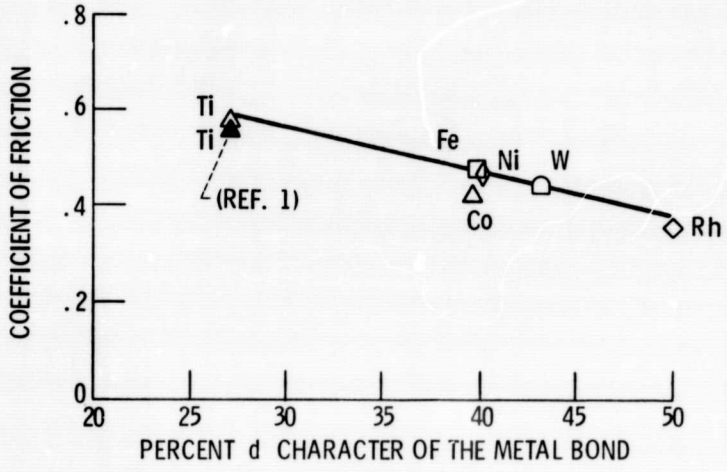

Figure 2. - Coefficient of friction as function of percent of metal d bond character for single-crystal silicon carbide (0001) surface in sliding contact with various metals in vacuum (10^{-8} N/m^2). Sliding direction, $\langle 10\bar{1}0 \rangle$; sliding velocity, 3 mm/min; load, 5 to 50 grams; temperature, 25° C.

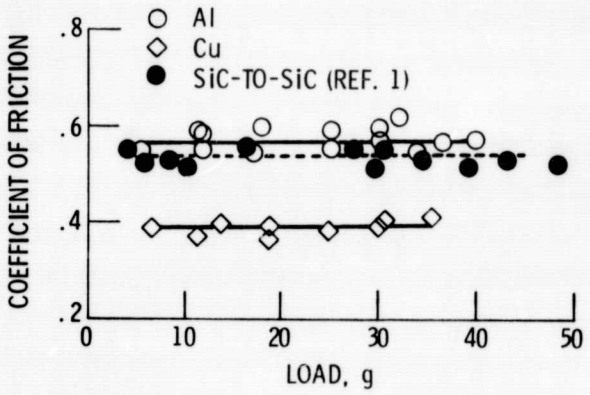

Figure 3. - Coefficient of friction as function of load for aluminum and copper sliding on single-crystal silicon carbide (0001) surface in vacuum (10^{-8} N/m^2 (P_a)). Sliding direction, $\langle 10\bar{1}0 \rangle$; sliding velocity, 3 mm/min; temperature, 25^0 C.

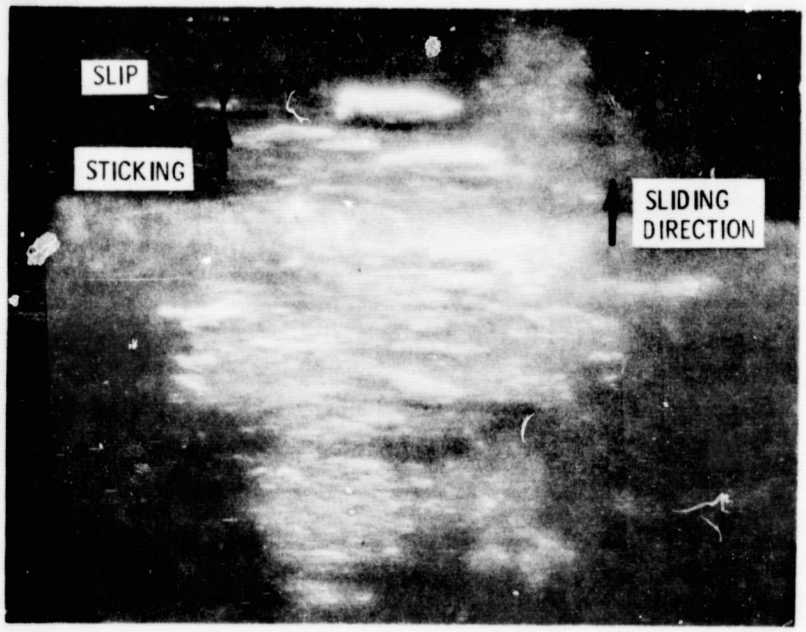

(a) METAL-TRANSFER TO SILICON CARBIDE (BEFORE GROSS SLIDING).

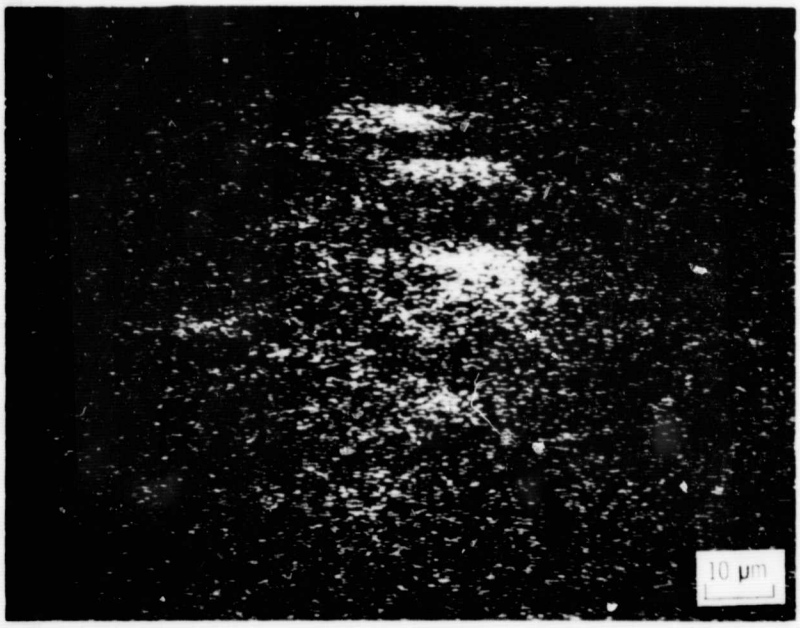

(b) ALUMINUM Kα X-RAY MAP; 1.5×10^4 COUNTS.

Figure 4. - Aluminum transferred to single-crystal silicon carbide as result of single pass of rider in vacuum (10^{-8} N/m^2). Scanning electron micrographs and x-ray map of a wear track or silicon carbide (0001) surface. Sliding direction, $\langle 10\bar{1}0 \rangle$; sliding velocity, 3 mm/min; load, 30 grams; temperature, 25° C.

E-9337

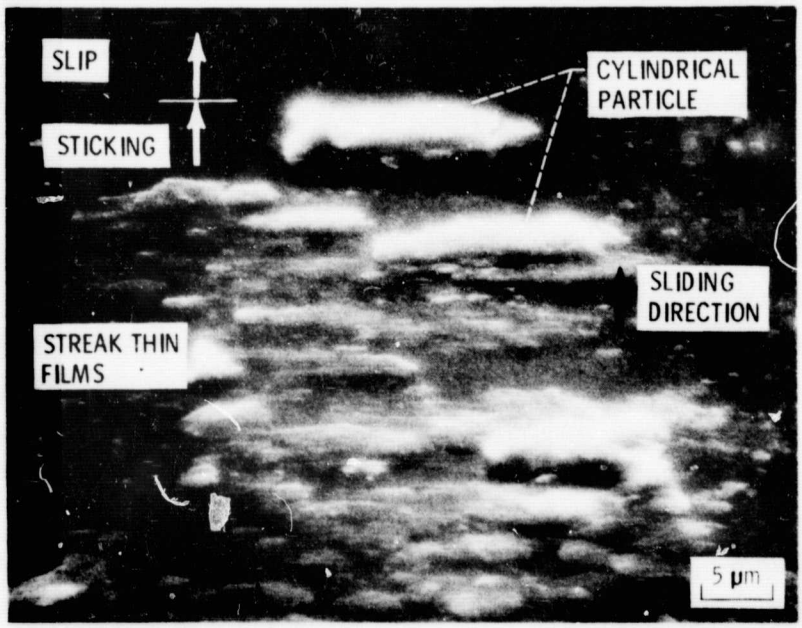

(c) WEAR DEBRIS OF ALUMINUM TRANSFERRED TO SILICON CARBIDE.

Figure 4. - Concluded.

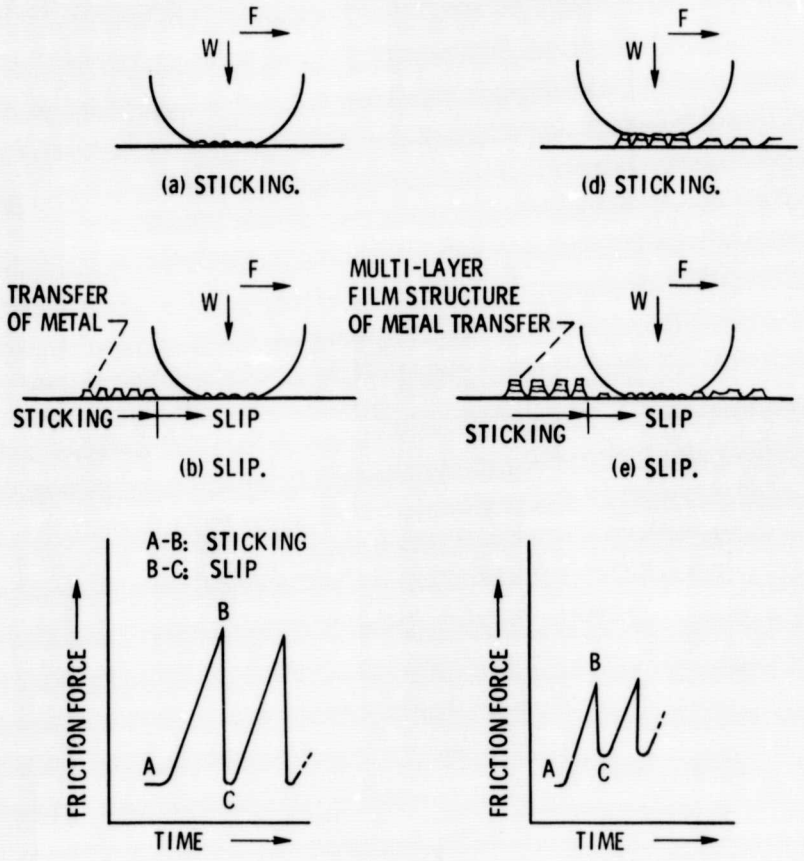

Figure 5. - Intermittent motion of friction and schematic model of metal transfer. Single and multi passes of aluminum rider on single-crystal silicon carbide (0001) surface; sliding direction, $\langle 10\bar{1}0 \rangle$; sliding velocity, 3 mm/min; load, 30 grams; temperature, 25^0 C and 10^{-8} N/m^2.

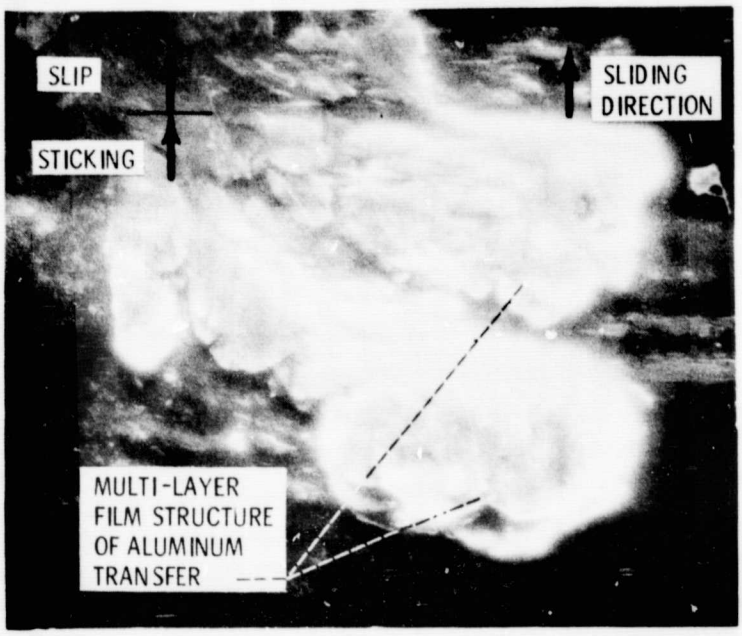

(a) METAL TRANSFER TO SILICON CARBIDE (BEFORE GROSS SLIDING).

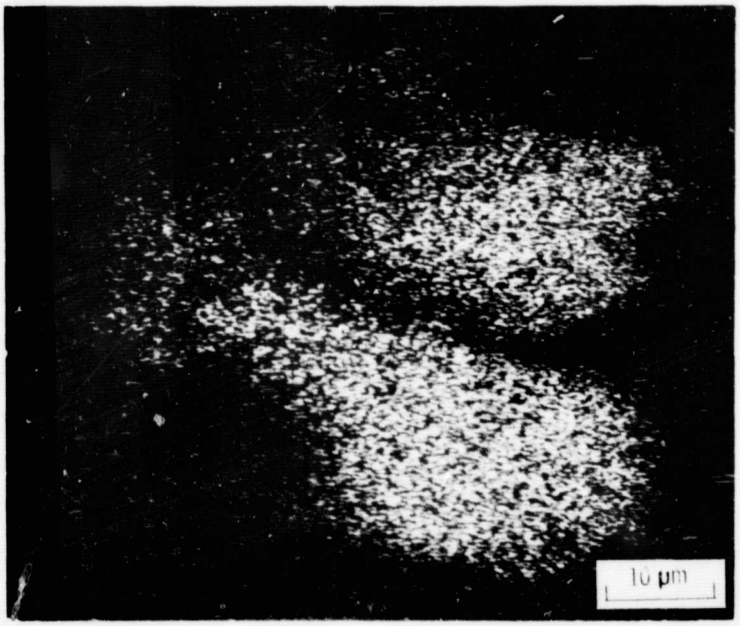

(b) ALUMINUM Kα X-RAY MAP; 1.5×10^4 COUNTS.

Figure 6. - Aluminum transferred to single-crystal silicon carbide as result of multi passes of rider in vacuum (10^{-8} N/m^2). Scanning electron micrograph and x-ray map of a wear track on silicon carbide (0001) surface. Sliding direction, $<10\bar{1}0>$; sliding velocity, 3 mm/min; load, 30 grams; temperature, 25° C.

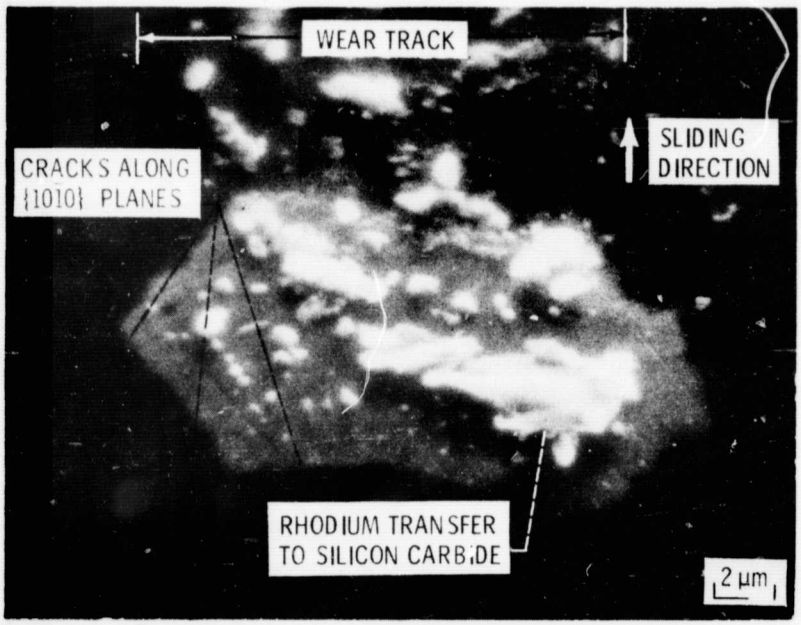

(a) SILICON CARBIDE-TO-RHODIUM CONTACT.

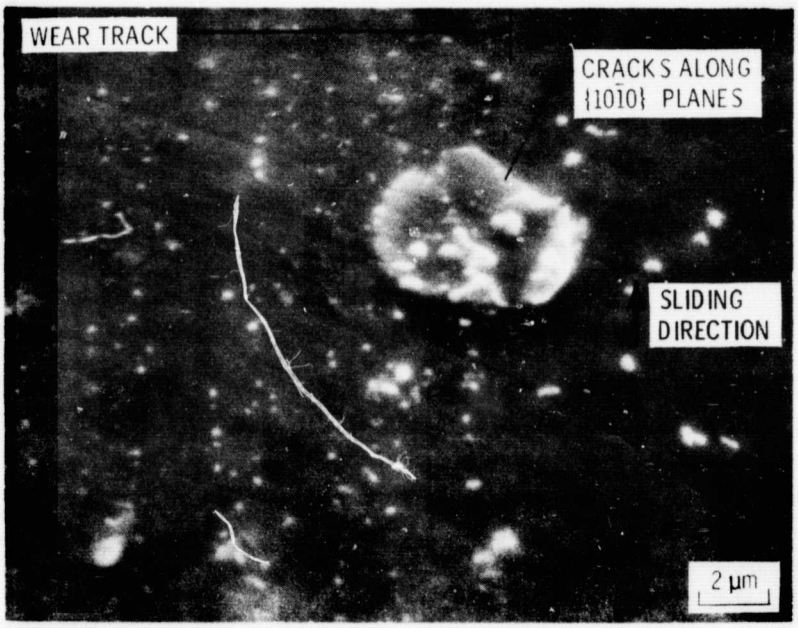

(b) SILICON CARBIDE -TO- COPPER CONTACT.

Figure 7. - Cracking of single-crystal silicon carbide in contact with rhodium and copper as result of ten passes of metal riders in vacuum (10^{-8} N/m^2). Scanning electron micrographs of wear tracks on silicon carbide (0001) surface. Sliding direction, <10$\bar{1}$0>; sliding velocity, 3 mm/min; load, 30 grams; temperature, 25^0 C.

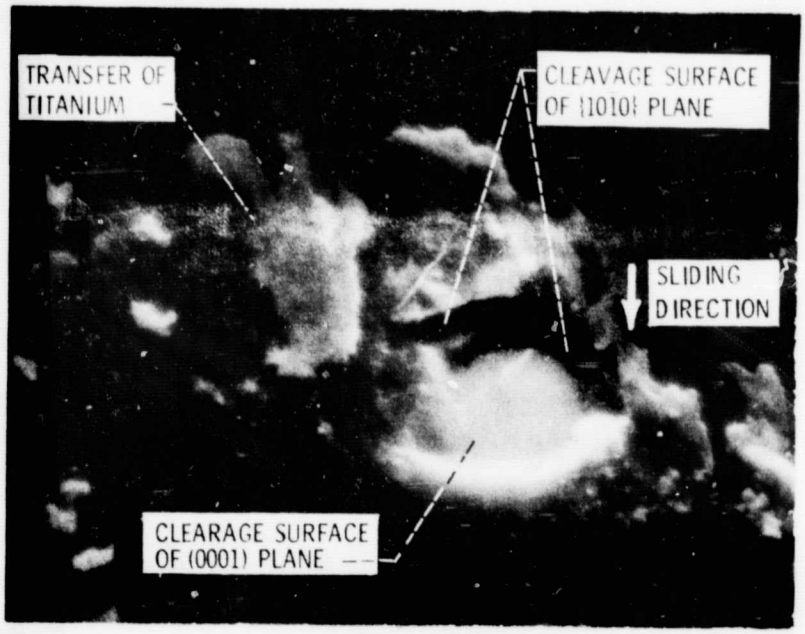

(a) NEARLY COMPLETE HEXAGON SHAPE PIT.

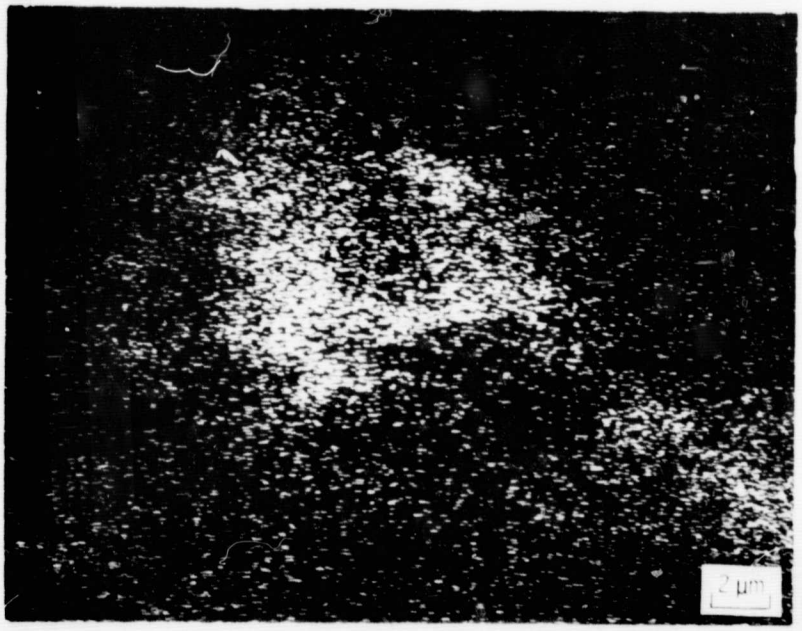

(b) TITANIUM, Kα X-RAY OF SILICON CARBIDE, 1.5×10^4 COUNTS.

Figure 8. - Hexagon shaped pit of single-crystal silicon carbide in contact with titanium as result of ten passes of rider in vacuum (10^{-8} N/m^2). Scanning electron micrograph and an x-ray dispersive analysis of a wear track on silicon carbide (0001) surface. Sliding velocity, 3 mm/min; load, 30 grams; temperature, 25° C.

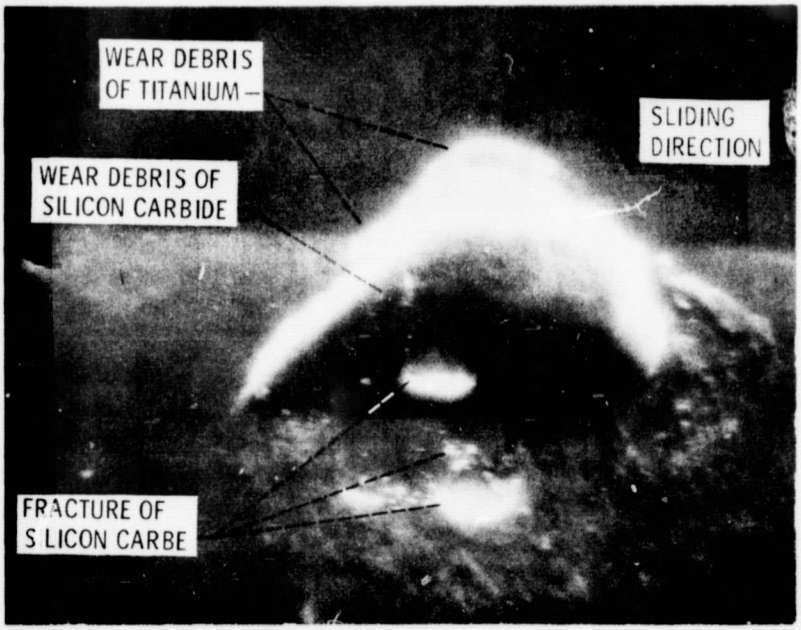

(a) TITANIUM AND SILICON CARBIDE WEAR DEBRIS.

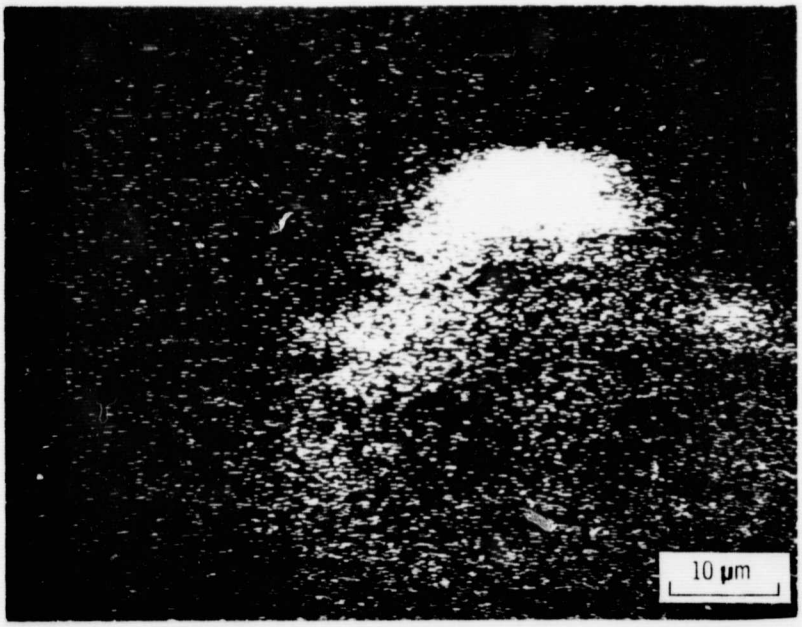

(b) TITANIUM Kα X-RAY MAP OF SILICON CARBIDE SURFACE; 1.5×10^4 COUNTS.

Figure 9. - Both titanium and silicon carbide wear debris produced as result of ten passes of rider in vacuum (10^{-8} N/m^2). Scanning electron micrograph and x-ray dispersive analysis of a wear track on silicon carbide (0001) surface. Sliding velocity, 3 mm/min; load, 30 grams; temperature, 25° C

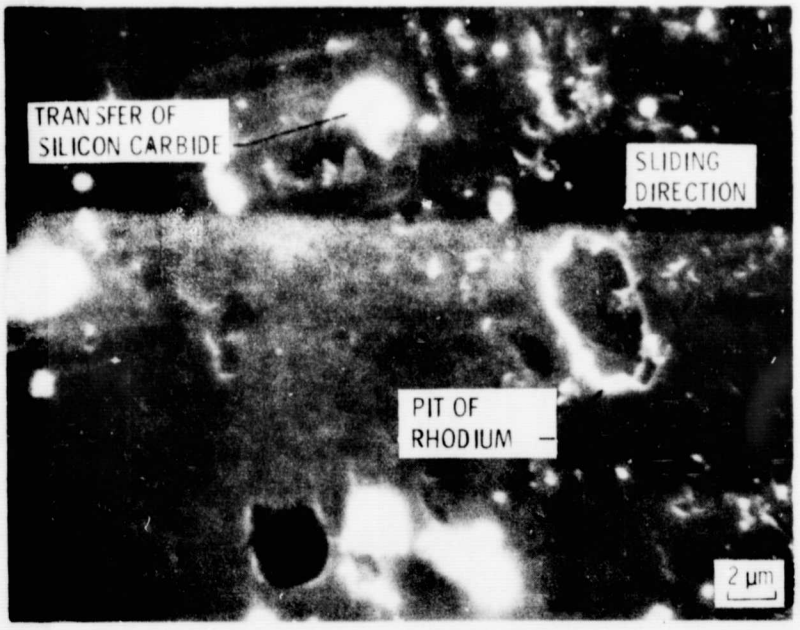

(a) PIT IN RHODIUM SURFACE AS RESULT OF TEN PASSES.

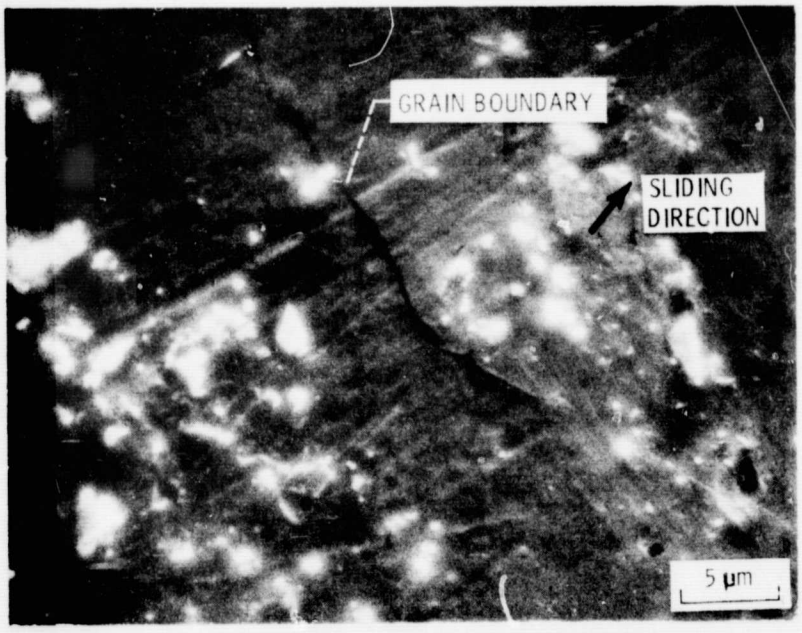

(b) CRACKS PROPAGATION ALONG GRAIN BOUNDARY AS RESULT OF THREE PASSES.

Figure 10. - Fractured surface damage and pitting as results of multiple passes of rhodium riders over the same silicon carbide (0001) surface in the $<10\bar{1}0>$ direction in vacuum (10^{-8} N/m^2). Scanning electron micrographs of wear scars on rhodium riders. Sliding velocity, 3mm/min; load, 30 grams; temperature 25^{0} C.

(a-1) SILICON CARBIDE WEAR DEBRIS.

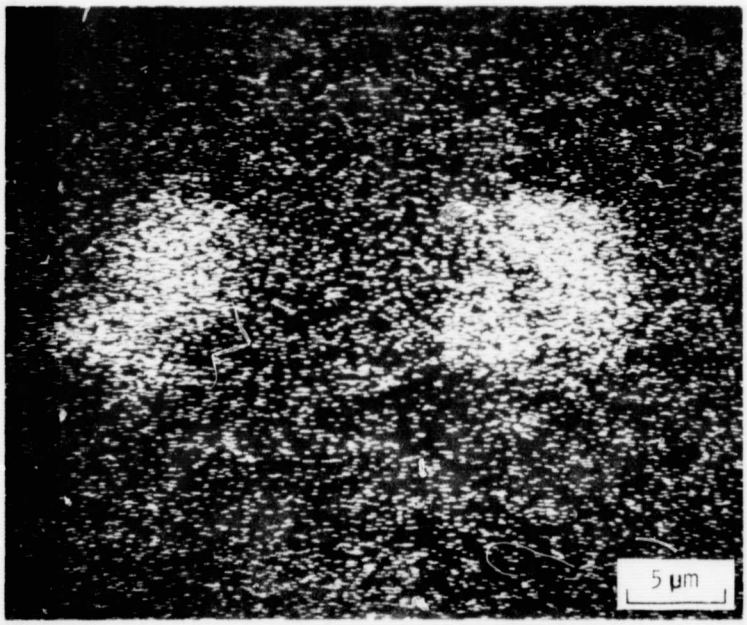

(a-2) SILICON, Kα X-RAY MAP OF RHODIUM RIDER; 2.0×10^4 COUNTS.

(a) SILICON CARBIDE WEAR DEBRIS ON RHODIUM RIDER.

Figure 11. - Silicon carbide wear debris, grooves and indentations on metals as results of ten passes of riders in vacuum (10^{-8} N/m^2). Scanning electron micrographs and an x-ray dispersive analysis of wear scars on metal riders. Sliding direction, $\langle 10\bar{1}0 \rangle$; sliding velocity, 3mm/min; load, 30 grams; temperature, 25° C.

(b) GROOVES ON COPPER RIDER.

(c) INDENTATIONS ON COBOLT RIDER PRODUCED BY ROLLING OF WEAR DEBRIS OF SILICON CARBIDE.

Figure 11. - Concluded.

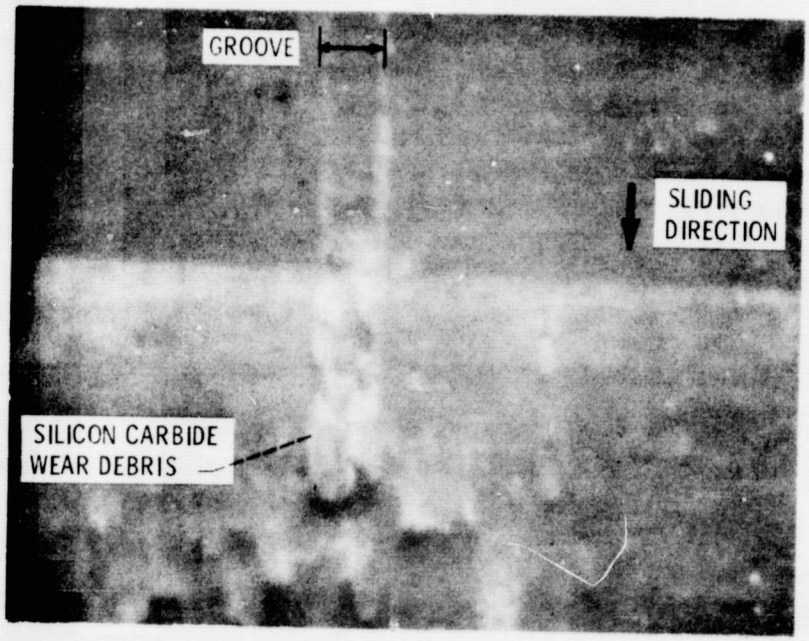

(a) GROOVE ON SILICON CARBIDE (0001) SURFACE.

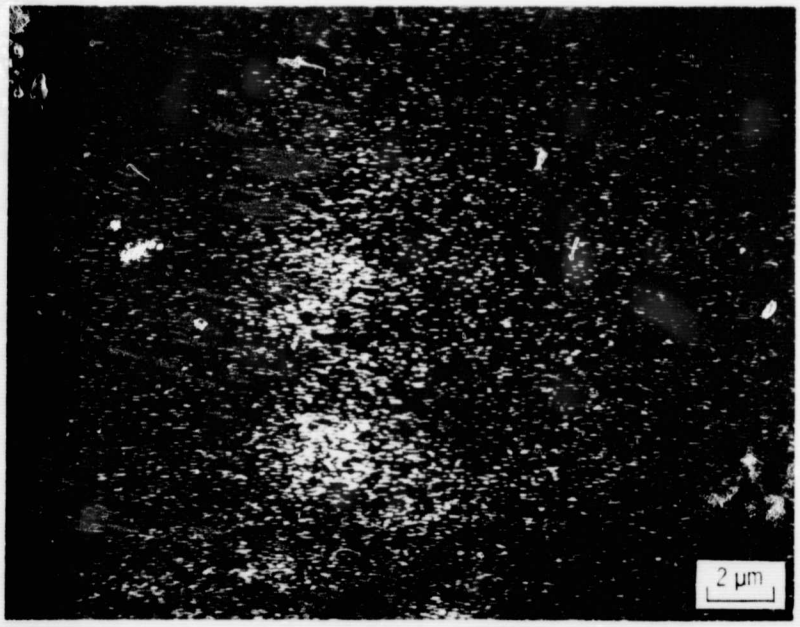

(b) TITANIUM Kα X-RAY MAP OF SILICON CARBIDE SURFACE, 1.7×10^4 COUNTS.

Figure 12. - Groove on silicon carbide (0001) surface produced by scratching of a wear debris of silicon carbide itself as result of ten passes of titanium rider on silicon carbide (0001) surface in vacuum (10^{-8} N/m^2). Scanning electron micrograph and x-ray dispersive analysis of wear track on silicon carbide surface. Sliding velocity, 3mm/min; load, 30 grams; temperature, 25° C.